Chinese Physics B

PAPER

Low-temperature heat transport of the zigzag spin-chain compound $SrEr_2O_4$

To cite this article: Liguo Chu *et al* 2022 *Chinese Phys. B* **31** 087505

Low-temperature heat transport of the zigzag spin-chain compound $SrEr_2O_4$

Liguo Chu(褚利国)[1], Shuangkui Guang(光双魁)[1], Haidong Zhou(周海东)[2], Hong Zhu(朱弘)[1], and Xuefeng Sun(孙学峰)[1,3,†]

[1] *Department of Physics, Key Laboratory of Strongly-Coupled Quantum Matter Physics (CAS), University of Science and Technology of China, Hefei* 230026, *China*

[2] *Department of Physics and Astronomy, University of Tennessee, Knoxville, Tennessee* 37996-1200, *USA*

[3] *Institute of Physical Science and Information Technology, Anhui University, Hefei* 230601, *China*

(Received 8 March 2022; revised manuscript received 16 March 2022; accepted manuscript online 17 March 2022)

Low-temperature thermal conductivity (κ), as well as the magnetic properties and specific heat, are studied for the frustrated zigzag spin-chain material $SrEr_2O_4$ by using single-crystal samples. The specific heat data indicate the long-range antiferromagnetic transition at ~ 0.73 K and the existence of strong magnetic fluctuations. The magnetizations at very low temperatures for magnetic field along the c axis (spin chain direction) or the a axis reveal the field-induced magnetic transitions. The κ shows a strong dependence on magnetic field, applied along the c axis or the a axis, which is closely related to the magnetic transitions. Furthermore, high magnetic field induces a strong increase of κ. These results indicate that thermal conductivity along either the c axis or the a axis are mainly contributed by phonons, while magnetic excitations play a role of scattering phonons.

Keywords: spin chain, quantum spin system, thermal conductivity

PACS: 75.50.–y, 75.50.Ee **DOI:** 10.1088/1674-1056/ac5e97

1. Introduction

Quantum effects are enhanced in those antiferromagnetic (AF) systems with small spins, low dimensionality or spin frustration. The famous quantum spin systems in low-dimensional cases are the $S = 1/2$ Heisenberg chain and the $S = 1$ Haldane chain, which can exhibit gapless spin liquid or spin gapped ground state.[1–4] Geometrically frustrated magnets, in which the magnetic interactions are incompatible with the underlying lattice symmetry, have attracted much attention. In such systems, the competitive interactions prohibit the energy-minimized local spin configuration from extending globally, and result in a macroscopically degenerate ground state in which many novel magnetic behaviors can emerge. Even in rare-earth compounds where the anisotropic moments induced by spin–orbit coupling are commonly regarded as the classical ones in the low temperature limit, with the help of magnetic frustration, some novel magnetic properties have been discovered experimentally.[5–7]

$SrEr_2O_4$ belongs to the family of isostructural magnetically frustrated compounds AB_2O_4 (A = Sr, Ba and B = lanthanide).[8] In these materials, the B ions are located inside two kinds of differently distorted oxygen octahedrons, resulting in two magnetically inequivalent B sites. In $SrEr_2O_4$, the two sets of Er magnetic moments form two different zigzag Ising spin chains along the c axis, which connect with each other to form a distorted honeycomb sublattice with the honeycomb layer perpendicular to the chain direction, as shown in Fig. 1. Thus, this material is a special one-dimensional and frustrated spin system. The intra-chain and inter-chain spin exchanges have not been determined experimentally. However, the magnetic susceptibility data demonstrated a rather large Curie–Weiss temperature θ_{CW} of -13.5 K, compared to the Néel temperature T_N of 0.75 K.[9] Actually, the previous studies revealed some unusual magnetic properties in $SrEr_2O_4$. At low temperatures there is the coexistence of AF long-range order (LRO) and incommensurate short-range order (SRO) involving Er1 sites and Er2 sites, respectively.[9,10] It was also determined that the magnetic moments on Er1 sites and Er2 sites point toward the c-axis and a-axis directions, respectively. For $B||a$, a 1/3 magnetization plateau was observed and indicated a field-induced two-spin-up one-spin-down (UUD) phase.[11]

It has been known that the heat transport of low-dimensional spin systems exhibit many interesting properties due to the possible transport of magnetic excitations and the spin–phonon scattering. In particular, large magnetic heat transport has been found in some one-dimensional and two-dimensional spin systems.[12–14] In some frustrated spin systems, the peculiar spinon excitations associated with the quantum spin liquid state have also been found to transport heat.[15–17] However, in more spin frustrated materials the magnetic excitation seems to scatter phonons rather than to carry heat.[18,19] In this work, we study the magnetic and heat-transport properties of $SrEr_2O_4$ single crystals by using

†Corresponding author. E-mail: xfsun@ustc.edu.cn

magnetic susceptibility, specific heat and thermal conductivity measurements at very low temperatures down to 0.3 K and in high magnetic fields up to 14 T. Thermal conductivity results indicate that phonons are the main heat carriers in this material, while magnetic excitations play a role of scattering phonons.

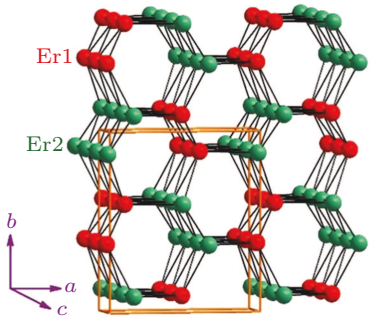

Fig. 1. Schematic plot of the crystal structure of $SrEr_2O_4$, in which Er ions on two inequivalent sites form two zigzag chains. The other atoms are omitted for clarity.

2. Experiment

High-quality $SrEr_2O_4$ single crystals were grown by using the floating-zone technique. The x-ray backscattering Laue photographs as well as x-ray diffraction were used for identifying the crystal quality and crystallographic directions. Large pieces of crystals were cut into long bar-shaped samples along the crystallographic axes for the thermal conductivity measurements, which were carried out in a ^{3}He refrigerator equipped with a 14-T magnet.[18,19] The specific heat was measured by the relaxation method in the temperature range from 0.4 K to 30 K on a physical property measurement system (PPMS, Quantum Design). Magnetization and magnetic susceptibility were measured using a Quantum Design superconducting quantum interference device with a vibrating sample magnetometer (SQUID-VSM), equipped with a ^{3}He refrigerator insert. For all measurements above, the magnetic field were applied along the a axis or c axis.

3. Results and discussion

3.1. Magnetic susceptibility and magnetization

Figure 2(a) shows the temperature dependence of magnetization $M(T)$ at 1.7 K to 0.45 K and in various magnetic fields along the c axis. In 0.01-T field, a clear drop of magnetization occurs at 0.75 K, which indicates an AF phase transition according to the previous works.[9,11] Below $T_N = 0.75$ K, the $M(T)$ curves tend to approach finite values as temperature decreases. The transition temperature decreases with increasing field to 0.1 T and meanwhile the drop becomes weaker. At $B = 0.4$ T the drop is replaced by a slope change of $M(T)$ at ~ 0.7 K. With further increasing field, the $M(T)$ curves display a monotonic increase with decreasing temperature, indicating that the Er1 sublattice enters a high-field polarized state.

Figure 2(b) shows the results of the zero-field cooling (ZFC) and field cooling (FC) data of $M(T)$ for $B||a$ at 0.45 K and 1 K. Spin freezing behavior in this material can be excluded since there is no significant difference between the FC and ZFC data. For $B = 0.1$ T, the $M(T)$ has a broad peak at 0.75 K, which is also due to the AF transition.

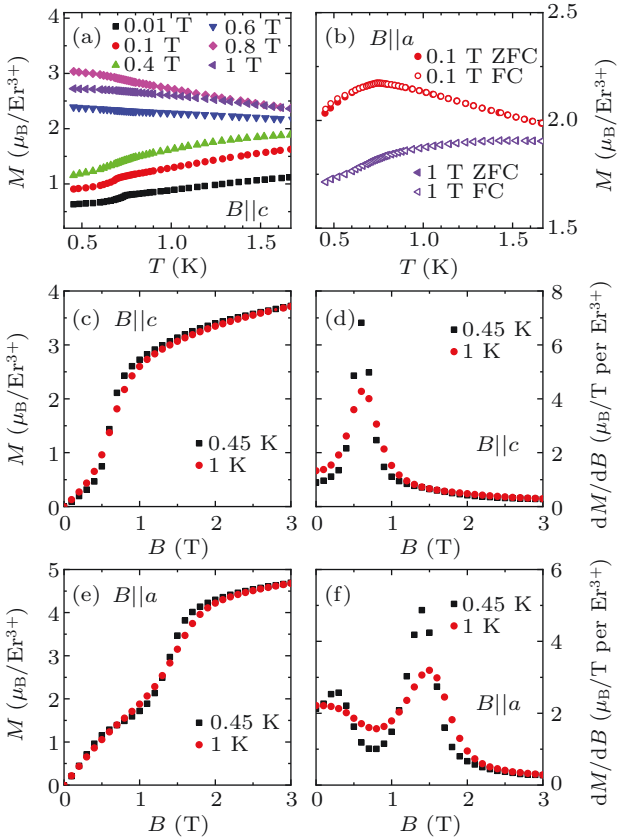

Fig. 2. (a) Magnetization measured at the temperature from 0.45 K to 1.7 K with various magnetic fields along the c axis. (b) Magnetization with fields along the a axis obtained both after ZFC and FC procedures. (c) and (e) Magnetization curves of $SrEr_2O_4$ single crystals at 0.45 K and 1 K with magnetic field along the c axis and a axis, respectively. (d) and (f) The differential curves of the magnetization dM/dB corresponding to panels (c) and (e).

Figures 2(c) and 2(e) show the magnetic field dependence of magnetization at very low temperatures for $B \parallel c$ and $B \parallel a$, which are highly nonlinear and exhibit strong anisotropy along two crystallographic directions. The $M(B)$ for $B \parallel c$ exhibits a sharp increase at 0.6 T, which is evidenced as a peak on the differential curve as shown in Fig. 2(d). This indicates a field-induced metamagnetic transition, which is sharper at lower temperature. Neutron diffraction measurements revealed that the magnetic moments point along the c axis and only one of the Er sites (Er1) carries a sizeable magnetic moment.[9] That is, the contribution to magnetization for $B \parallel c$ is mainly from the Er1 sublattice, with only a small component of Er2 moments canted along the magnetic field direction. As reported previously,[9] the Er1 moments form ferromagnetic chains along the c axis and the adjacent chains couple antiferromagnetically. At 0.55 K, the magnetic moment on the Er1 site has an average magnitude of 4.5 μ_B,[9] while the mag-

netic moment per Er^{3+} ion after the metamagnetic transition is $\sim 2.2\ \mu_B$, which reaches the half value of the Er1 moment. Therefore, the 0.6-T transition should be a spin-flip transition to the polarized phase of the Er1 sublattice.

For $B||a$, the $M(B)$ curves exhibit two quick increases with a plateau-like feature, indicated by two maxima at about 0.3 T and 1.4 T in the 0.45 K differential curve as shown in Fig. 2(f). It is notable that the region of the plateau narrows as the temperature decreases. This means that the UUD phase is stabilized partially due to the thermal fluctuations, while in such a highly frustrated magnet the quantum fluctuations cannot be excluded.

3.2. Specific heat

Figure 3 shows the temperature dependence of specific heat of $SrEr_2O_4$ single crystal in various magnetic fields along two different crystallographic axes. The zero-field data shows a sharp λ-type peak at $T_N \sim 0.73$ K, which is attributed to the long-range AF transition.[9] Besides, there is a large broad peak at low temperatures, indicating significant magnetic contributions from the short-range spin correlation or crystal field effect (CEF) of Er^{3+} ions.

In order to extract the magnetic contribution to the low-temperature specific heat, other terms such as phonon specific heat (C_{ph}), nuclear Schottky specific heat (C_n), and crystal field Schottky specific heat (C_{CEF}) should be determined and subtracted from the measured data. The nuclear Schottky specific heat from Er^{3+} nuclear moment is negligibly small in the present temperature range,[20,21] hence it could be ignored without causing considerable errors. It is known that the Er^{3+} multiplet $^4I_{15/2}$ splits into eight Kramers doublets in the distorted octahedral crystal field.[22] Therefore, we take these low-lying CEF energy levels to calculate C_{CEF} by using a multi-level Schottky specific heat expression:[23]

$$C_{CEF} = R\frac{\sum_i\sum_j g_i g_j \varepsilon_i(\varepsilon_i-\varepsilon_j)\exp[-(\varepsilon_i+\varepsilon_j)/k_BT]}{[k_BT\sum_i g_i \exp(-\varepsilon_i/k_BT)]^2}, \quad (1)$$

where ε_i or ε_j $(i, j = 0, 1, 2, 3, 4)$ is one of the five lower sublevels of the splitting $^4I_{15/2}$ multiplet of which the magnitudes were determined in Ref. [14], g_i or g_j is the degeneracy of each energy level, and R is the universal gas constant. Two sets of the crystal field energy levels for the two crystallographically inequivalent Er^{3+} ions were substituted into Eq. (1) to calculate their C_{CEF}, as shown in Figs. 3(a) and 3(c). After subtracting the CEF contribution, the remaining terms of specific heat are plotted in Figs. 3(b) and 3(d).

To further subtract the contribution of phonons C_{ph}, a truncated odd-order Taylor series expansion $C_{ph}(T) = \beta_3 T^3 + \beta_5 T^5 + \beta_7 T^7$ was used to fit the zero-field data at high temperatures.[24] The results of fitting are shown by the black dashed lines in Figs. 3(b) and 3(d). Based on the approximation formula $\beta_3 = (12/5)\pi^4 n_A R/(\theta_D)$, the obtained fitting parameter $\beta_3 = 1.52 \times 10^{-4}$ J/K^4·mol gives a Debye temperature $\Theta_D = 447$ K, which is comparable to that (460 K) obtained from the thermal expansion experiment.[25] Here, n_A is the number of atoms in each molecule.

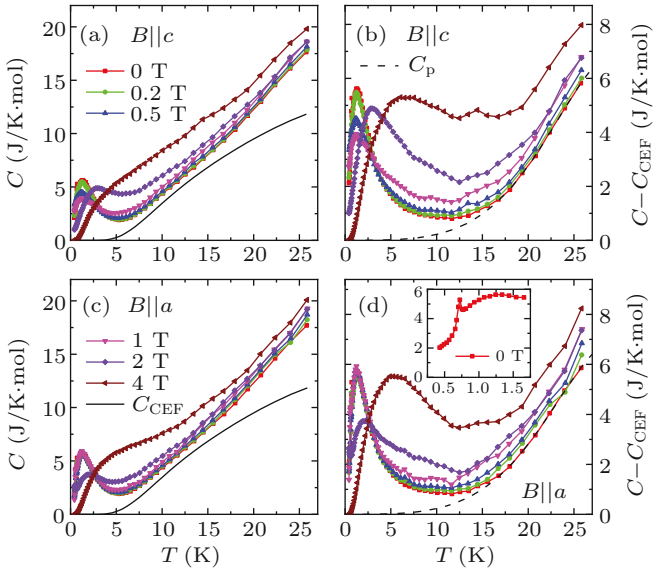

Fig. 3. Low temperature specific heat of $SrEr_2O_4$ single crystals measured with magnetic field $B \parallel c$ (a) and $B \parallel a$ (c). C_{CEF} is the calculated CEF specific heat which is described in details in the main text. (b) and (d) Remaining specific heat after subtracting the CEF contribution for $B \parallel c$ and $B \parallel a$, respectively. The black dashed lines show the fitted results of phonon specific heat by using a Taylor series expansion. Inset: the zoom-in of the low-temperature data at zero field.

The magnetic contribution to specific heat C_m is obtained using $C_m = C - C_{CEF} - C_{ph}$ and is plotted in Fig. 4. At zero field, besides the small and sharp λ-type peak at $T_N \sim 0.73$ K, there is a broad peak at ~ 1.3 K, which should be related to the development of the incommensurate short-range magnetic order.[9] For $B \parallel c$, the λ-type peak is completely smeared out by a magnetic field as low as 0.2 T. The broad peak shifts slightly to lower temperature with applying weak fields (≤ 1 T), which rules out the possibility of the Schottky origin. For $B \parallel a$, as the magnetic field increases the λ peak shifts to lower temperatures, which is a typical result for an AF system. At the same time, the peak becomes lower and broader but is still discernible with increasing field up to 1 T. It is worth noting that the broad peak does not change with applying weak magnetic fields (≤ 1 T) but is strongly affected by higher fields. Nevertheless, the magnetic specific heat data indicate strong magnetic fluctuations in this low-dimensional spin system.

$SrEr_2O_4$ belongs to a family of geometrically frustrated magnets with the chemical formula AB_2O_4, most of which can be described by the one-dimensional (1D) axial next-nearest neighbor Ising (ANNNI) model.[26,27] Indeed, $SrEr_2O_4$ shows some characteristics of 1D ANNNI model, such as a double Néel ground state and a 1/3 magnetization plateau in

the intermediate field.[28–30] However, the rigorous ANNNI model may not be fully applicable to $SrEr_2O_4$. Theoretical calculation and experimental results verified the existence of a specific heat peak whose position changes with magnetic field.[31–33] This is a bit different from what we observed in $SrEr_2O_4$.

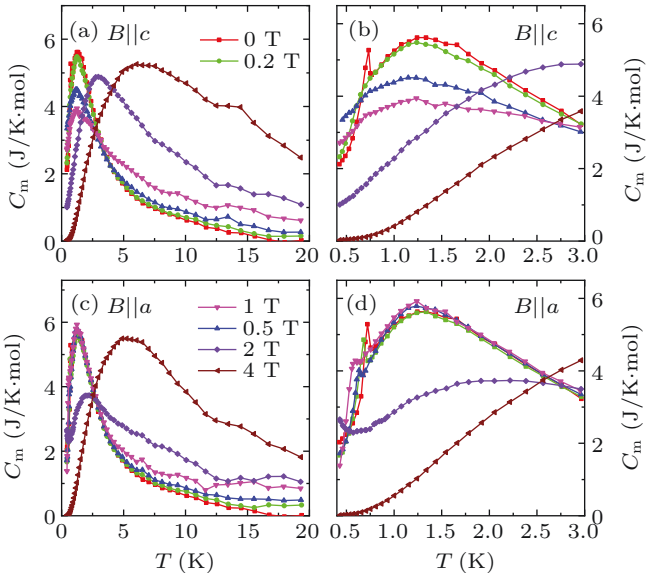

Fig. 4. Magnetic specific heat of $SrEr_2O_4$ in various magnetic fields for $B \parallel c$ (a) and $B \parallel a$ (c). (b) and (d) Zoom in of data for $T < 3$ K.

3.3. Thermal conductivity

Figure 5 shows the temperature dependence of thermal conductivity κ of $SrEr_2O_4$ single crystals in various magnetic fields with heat current along the a axis or c axis and at temperatures from 0.3 K to 30 K. The inset shows the comparison of κ_a and κ_c in zero field. They show a nearly isotropic behavior except for slight difference at low temperatures. Since $SrEr_2O_4$ has a low-dimensional spin system, in which the exchange coupling along the c axis is much stronger than that along the a axis, the isotropic heat transport indicates that the spin excitations mainly play a role of scattering phonons rather than carrying heat. This is further confirmed by the strong increase of κ in high magnetic fields, which can be attributed to the suppression of magnetic excitations by high fields. At very low temperatures, the phonon thermal conductivity tends to follow a T^3 temperature dependence known as the boundary scattering limit.[34] Hence, the change of the zero-field $T^{1.5}$ power law dependence of κ_c to $T^{2.5}$ in 14-T field, as shown in Fig. 5(c), demonstrates that the magnetic excitations scattering of phonon is significantly suppressed by such a large magnetic field, and the T^3 behavior tends to be established. Another feature of the zero-field $\kappa(T)$ data is the kink around 1.2 K, which has some correspondence to the broad peak of magnetic specific heat. Apparently, the magnetic fluctuations evidenced by the specific heat can induce strong scattering of phonons.[35–38]

Figures 6 and 7 show the low-temperature magnetic field dependences of κ_a and κ_c, respectively, for fields up to 14 T. A notable result is that the field dependence of κ is mainly determined by the field direction rather than heat current direction, which can be attributed to the anisotropic magnetic properties. This also indicates that there is no sizeable magnetic heat transport in this low-dimensional spin system.

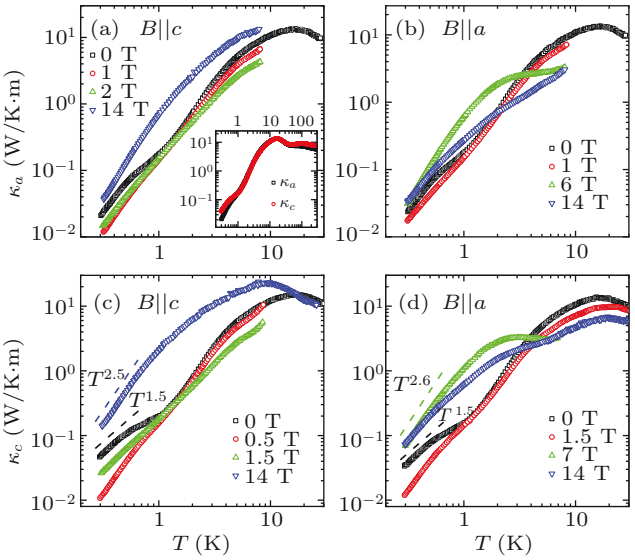

Fig. 5. Temperature dependences of thermal conductivity along the a axis (κ_a) and that along the c axis (κ_c) of $SrEr_2O_4$ single crystals for magnetic field applied along either the a axis or the c axis. The inset shows the zero-field κ_a and κ_c for comparison.

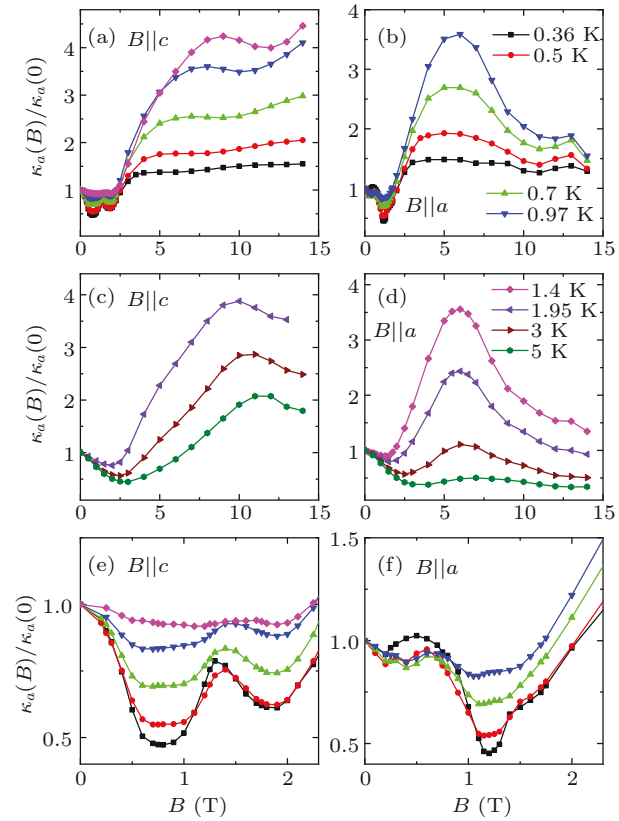

Fig. 6. Magnetic field dependences of κ_a at low temperatures with field applied along either the a axis or c axis.

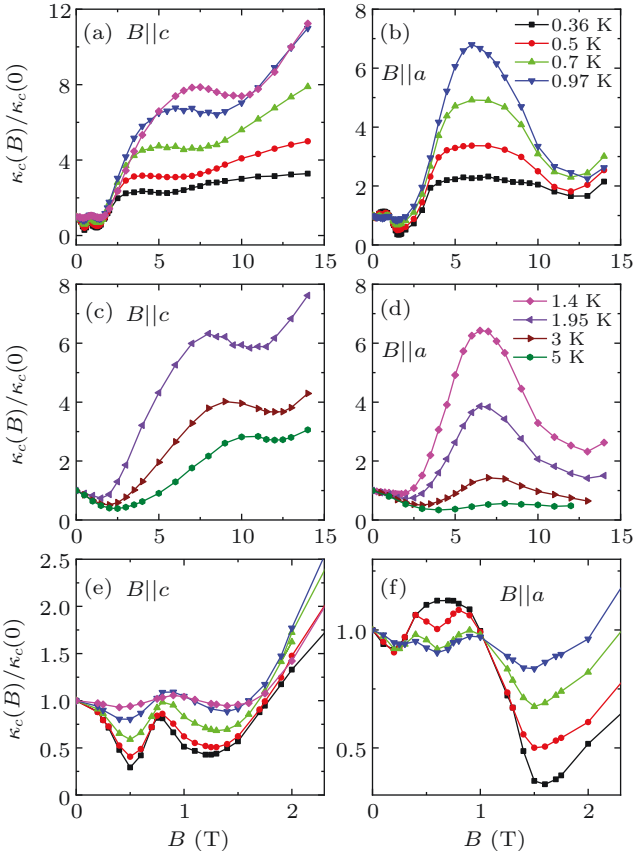

Fig. 7. Magnetic field dependences of κ_c at low temperatures with field applied along either the *a* axis or *c* axis.

For $B \parallel c$, the $\kappa_a(B)$ and $\kappa_c(B)$ isotherms display two dips at low fields, followed by a quick increase at high fields. The first dip becomes sharper with the position unchanged upon lowering temperature. It corresponds to the field-induced phase transition of the Er1 sublattice. Similar phenomena have been observed in many other materials.[35–38] The second dip should be also related to the Er1 sublattice. However, its position slightly moves to higher field with increasing temperature, accompanied with the weakening of the dip at 0.36 K–1.4 K. With further increasing temperature, these two dips disappears and another broad dip appears. The position of this new dip moves to higher field associated with deeper value, which suggests that it may be caused by the resonant phonon scattering by Er^{3+} CEF energy levels or magnetic fluctuations.[39–42]

For $B \parallel a$, the $\kappa_a(B)$ and $\kappa_c(B)$ isotherms display a bit more complicated behavior. At the lowest temperature of 0.36 K, the $\kappa_a(B)$ and $\kappa_c(B)$ curves have two dips at 0.2, 1.2 T and 0.2, 1.6 T, respectively, which can be related to the low- and high-field boundaries of the UUD phase. Theoretically, the UUD phase has a magnetic excitation gap, which approaches zero at both ends of the UUD phase and maximizes in the middle.[43] Thus, at the phase boundaries phonons are strongly scattered by the enhanced magnetic excitations, leading to two dips on the $\kappa_a(B)$ curve. At 0.5 K–0.97 K, there is another unexpected dip appearing at 0.6 T, whose origin is not clear now. Similar phenomenon has been observed in a triangular-lattice magnetic system $Ba_3CoSb_2O_9$.[36,44] The authors interpreted it as an unknown magnetic state change inside the UUD state. At these temperatures, there is a much deeper minimum at about 1.6 T, which can be attributed to the transition to the spin polarized state. At higher temperatures ($T \geq 1.4$ K), these dips disappear and another broad dip associated with phonon resonant scattering appears.

It should be pointed out for either $B \parallel c$ or $B \parallel a$, the low-temperature $\kappa(B)$ curves reach much larger values at high field than that at zero field. This indicates that at zero field there are rather strong magnetic scattering of phonons, which can be suppressed by high magnetic fields. Furthermore, the $\kappa(B)$ curves are not simply saturated at high fields and display some broad valley-like behavior. This indicates that the magnetic fluctuations are so strong in this system that 14-T field may not be strong enough to completely suppress them. Another possibility is related to the phonon resonant scattering of higher CEF energy levels.[39,40]

All the above temperature dependence and magnetic field dependence of κ demonstrate that in $SrEr_2O_4$ the magnetic excitations play a role of scattering phonons rather than carry heat. It is different from many other low-dimensional spin systems.[12–14] In particular, both the experimental and theoretical studies revealed ballistic spin transport in some spin-chain and spin-ladder materials.[12–14] To our knowledge, there is no theoretical studies on the magnetic heat transport of zigzag spin-chain compounds. The results in this work provide new experimental information on the heat transport of this one-dimensional and frustrated spin system and the theoretical investigation is called for.

4. Summary

In summary, the thermal conductivity, magnetic susceptibility, and specific heat at very low temperatures are studied for $SrEr_2O_4$ single crystals, which is known as a frustrated zigzag spin chain system. The magnetic field induced magnetic transitions for either $B||c$ or $B||a$ are characterized by magnetization results, while the specific heat data indicates strong spin fluctuations at low temperature. The thermal conductivity shows strong magnetic field dependence, indicating the strong coupling between phonons and magnetic excitations. At very low temperatures, the magnetic transitions induce minima at the $\kappa(B)$ isotherms and high magnetic field induces a strong increase of κ. These results indicate that the low-temperature thermal conductivity of this material are mainly contributed by phonons, while magnetic excitations play a role of scattering phonons.

Acknowledgements

We thank Jichuan Wu for helps on experiments. Project supported by the National Natural Science Foundation of

China (Grant Nos. U1832209 and 11874336). The work at the University of Tennessee (H D Zhao) was supported by the NSF with Grant No. NSF-DMR-2003117.

References

[1] Haldane F D M 1983 *Phys. Rev. Lett.* **50** 1153
[2] Haldane F D M 1983 *Phys. Lett. A* **93** 464
[3] Fan Y and Yu R 2020 *Chin. Phys. B* **29** 057505
[4] Zhao B, Takahashi J and Sandvik A W 2020 *Chin. Phys. B* **29** 057506
[5] Wu L S, Gannon W J, Zaliznyak I A, Tsvelik A M, Brockmann M, Caux J S, Kim M S, Qiu Y, Copley J R D, Ehlers G, Podlesnyak A and Aronson M C 2016 *Science* **352** 1206
[6] Shen Y, Li Y D, Wo H, Li Y, Shen S, Pan B, Wang Q, Walker H C, Steffens P, Boehm M, Hao Y Q, Quintero-Castro D L, Harriger L W, Frontzek M D, Hao L, Meng S Q, Zhang Q M, Chen G and Zhao J 2016 *Nature* **540** 559
[7] Castelnovo C, Moessner R and Sondhi S 2008 *Nature* **451** 42
[8] Karunadasa H, Huang Q, Ueland B G, Lynn J W, Schiffer P, Regan K A and Cava R J 2005 *Phys. Rev. B* **71** 144414
[9] Petrenko O A, Balakrishnan G, Wilson N R, de Brion S, Suard E and Chapon L C 2008 *Phys. Rev. B* **78** 184410
[10] Hayes T J, Balakrishnan G, Deen P P, Manuel P, Chapon L C and Petrenko O A 2011 *Phys. Rev. B* **84** 174435
[11] Hayes T J, Young O, Balakrishnan G and Petrenko O A 2012 *J. Phys. Soc. Jpn.* **81** 024708
[12] Zhao X, Zhao Z Y, Liu X G and Sun X F 2016 *Sci. China-Phys. Mech. Astron.* **59** 117501
[13] Hess C 2007 *Eur. Phys. J. Spec. Top.* **151** 73
[14] Sologubenko A V, Lorenz T, Ott H R and Friemuth A 2007 *J. Low Temp. Phys.* **147** 387
[15] Yamashita M, Nakata N, Senshu Y, Masaki N, Yamamoto H M, Kato R, Shibauchi T and Matsuda Y 2010 *Science* **328** 1246
[16] Li N, Huang Q, Yue X Y, Chu W J, Chen Q, Choi E S, Zhao X, Zhou H D and Sun X F 2020 *Nat. Commun.* **11** 4216
[17] Rao X, Hussain G, Huang Q, Chu W J, Li N, Zhao X, Dun Z, Choi E S, Asaba T, Chen L, Li L, Yue X Y, Wang N N, Cheng J G, Gao Y H, Shen Y, Zhao J, Chen G, Zhou H D and Sun X F 2021 *Nat. Commun.* **12** 4949
[18] Li Q J, Zhao Z Y, Fan C, Zhang F B, Zhou H D, Zhao X and Sun X F 2013 *Phys. Rev. B* **87** 214408
[19] Gu C C, Zhao Z Y, Chen X L, Lee M, Choi E S, Han Y Y, Ling L S, Pi L, Zhang Y H, Chen G, Yang Z R, Zhou H D and Sun X F 2018 *Phys. Rev. Lett.* **120** 147204
[20] Che H L, Zhao Z Y, Rao X, Chu L G, Li N, Chu W J, Gao P, Yue X Y, Zhou Y, Li Q J, Huang Q, Choi E S, Han Y Y, He Z Z, Zhou H D, Zhao X and Sun X F 2020 *Phys. Rev. Materials* **4** 054406
[21] de Réotier P D, Yaouanc A, Chapuis Y, Curnoe S H, Grenier B, Ressouche E, Marin C, Lago J, Baines C and Giblin S R 2012 *Phys. Rev. B* **86** 104424
[22] Malkin B Z, Nikitin S I, Mumdzhi I E, Zverev D G, Yusupov R V, Gilmutdinov I F, Batulin R, Gabbasov B F, Kiiamov A G, Adroja D T, Young O and Petrenko O A 2015 *Phys. Rev. B* **89** 094415
[23] Mariano S, Ricardo P, Antonio S and Roberto E L 2016 *Braz. J. Phys.* **46** 206
[24] Tari A 2003 *Specific Heat of Matter at Low Temperatures* (London: Imperial College Press)
[25] Li H F, Wildes A, Hou B, Zhang C, Schmitz B, Meuffels P, Roth G and Bruckel T 2014 *RSC Adv.* **4** 53602
[26] Fennell A, Pomjakushin V Y, Uldry A, Delley B, Prévost B, Désilets-Benoit A, Bianchi A D, Bewley R I, Hansen B R, Klimczuk T, Cava R J and Kenzelmann M 2014 *Phys. Rev. B* **89** 224511
[27] Prévost B, Gauthier N, Pomjakushin V Y, Delley B, Walker H C, Kenzelmann M and Bianchi A D 2018 *Phys. Rev. B* **98** 144428
[28] Selke W 1988 *Phys. Rep.* **170** 213
[29] Gauthier N, Fennell A, Prvost B, Uldry A C, Delley B, Sibille R, Dsilets-Benoit A, Dabkowska H A, Nilsen G J, Regnault L P, White J S, Niedermayer C, Pomjakushin V, Bianchi A D and Kenzelmann M 2017 *Phys. Rev. B* **95** 134430
[30] Wen J J, Tian W, Garlea V O, Koohpayeh S M, McQueen T M, Li H F, Yan J Q, Rodriguez-Rivera J A, Vaknin D and Broholm C L 2015 *Phys. Rev. B* **91** 054424
[31] Kassan-ongly F A 2001 *Phase Transitions* **74** 353
[32] Taherkhani F, Daryaei E, Abroshan H, Akbarzadeh H, Parsafar G and Fortunelli A 2011 *Phase Transitions* **84** 77
[33] Cheffings T H, Lees M R, Balakrishnan G and Petrenko O A 2013 *J. Phys.: Condens. Matter* **25** 256001
[34] Berman R 1976 *Thermal Conduction in Solids* (Oxford: Oxford University Press)
[35] Li N, Huang Q, Brassington A, Yue X Y, Chu W J, Guang S K, Zhou X H, Gao P, Feng E X, Cao H B, Choi E S, Sun Y, Li Q J, Zhao X, Zhou H D and Sun X F 2021 *Phys. Rev. B* **104** 104403
[36] Fortune N A, Huang Q, Hong T, Ma J, Choi E S, Hannahs S T, Zhao Z Y, Sun X F, Takano Y and Zhou H D 2021 *Phys. Rev. B* **103** 184425
[37] Zhao Z Y, Li Q J, Liu X G, Rao X, Che H L, Chu L G, He Z Z, Zhao X and Sun X F 2019 *Phys. Rev. B* **99** 224428
[38] Song J D, Wang X M, Zhao Z Y, Wu J C, Zhao J Y, Liu X G, Zhao X and Sun X F 2017 *Phys. Rev. B* **95** 224419
[39] Sun X F, Tsukada I, Suzuki T, Komiya S and Ando Y 2005 *Phys. Rev. B* **72** 104501
[40] Sun X F, Taskin A A, Zhao X, Lavrov A N and Ando Y 2008 *Phys. Rev. B* **77** 054436
[41] Mcclintock P V E, Morton I P, Orbach R and Rosenberg H M 1967 *Proc. R. Soc. London, Ser. A* **298** 359
[42] Metcalfe M J and Rosenberg H M 1972 *J. Phys. C* **5** 450
[43] Lacroix C, Mendels P and Mila F 2011 *Introduction to Frustrated Magnetism: Materials, Experiments, Theory*, Vol. 164 (New York: Springer)
[44] Naruse K, Kawamata T, Ohno M, Matsuoka Y, Sudo H, Nagasawa H, Hagiya Y, Sasaki T and Koike Y 2014 *J. Phys.: Conf. Ser.* **568** 042014